

Engineering Notes

ENGINEERING NOTES are short manuscripts describing new developments or important results of a preliminary nature. These Notes should not exceed 2500 words (where a figure or table counts as 200 words). Following informal review by the Editors, they may be published within a few months of the date of receipt. Style requirements are the same as for regular contributions (see inside back cover).

Close-Formation Flight Control with Motion Synchronization

Jinjun Shan* and Hong-Tao Liu†

University of Toronto, Toronto, Ontario M3H 5T6, Canada

Introduction

FORMATION flight of multiple aircraft has been an active research topic for many years. For the classical lead–follower configuration, when the follower is properly positioned with respect to the lead, the drag on the follower aircraft can be remarkably reduced due to strong wingtip vortices generated by the lead aircraft. Such close-formation flight configurations can lead to reduction in fuel consumption and, thus, an increase in flight range. Previous formation flight of a pair of Dryden F/A-18s shows a 20% drag reduction and 18% fuel saving.¹

The high efficiency of close-formation flight relies on accurate relative position control between the follower and the lead aircraft, especially under the effect of coupled aerodynamics. Many control strategies have been proposed to treat close-formation flight with consideration of coupled aerodynamics.^{2,3}

In this Note, a motion synchronization control strategy is proposed to synchronize the relative position tracking motion between multiple follower aircraft. The NASA–Hallock–Burnham vortex profile is adopted to calculate the vortex-induced forces and moments. The autopilot models of the followers are modified with consideration of the coupled aerodynamics. Finally, the simulation results demonstrate the effectiveness and performance improvement with the proposed control method.

Vortex-Induced Aerodynamics

Figure 1 is a schematic diagram of formation flight. As shown in Fig. 1a, the formation geometry between the lead and follower aircraft can be described by three relative coordinates: the longitudinal separation x , the lateral separation y , and the vertical separation z .

The dynamics of aircraft in close-formation flight are much more complicated when compared with the dynamics in free flight due to aerodynamic interaction that arises from the vortex generated by the lead. Because this formation flight phenomenon significantly alters the follower dynamics, its effect has to be sufficiently captured in modeling for controller design, to ensure reliable performance of the control system in the real operating environment.

For close-formation flight, the impact of the longitudinal separation x on the induced forces and moments is much smaller than the

lateral separation y and the vertical separation z (Ref. 3). Therefore, we neglect the effect of the longitudinal separation x in vortex-induced aerodynamics modeling without the loss of significance. Furthermore, we assume that the lead and follower aircraft fly in parallel almost all of the time and there is no attitude difference between them, or the difference is small enough to be tracked quickly.

The tangential velocity $V_\theta(r)$ is frequently used to model a vortex in the rolled-up wake behind an aircraft. Here, we adopt the following NASA–Hallock–Burnham profile because it correlates well with experimental data (see Refs. 3 and 4):

$$V_\theta(r) = (\Gamma/2\pi r) \left[r^2 / (r^2 + r_c^2) \right] \quad (1)$$

where r is the radius from the vortex center, r_c is the core radius of the vortex, $\Gamma = Mg/\rho V b_0$ is the circulation that describes the vortex strength, Mg is the weight of aircraft, V is aircraft velocity, ρ is the air density at flight altitude h , b is wingspan, and $b_0 = \pi b/4$ is the displacement between the vortex pair.

Figure 1b shows the tangential velocities $V_{R\theta}$ and $V_{L\theta}$ of the right and the left vortex, respectively, at point P . These tangential velocities can be decomposed into upwash w and sidewash v . The vortex-induced upwash w changes the velocity vector of the follower aircraft. This change translates into an increase in the angle of attack and, thus, the lift. Therefore, the upwash w leads to changes in lift (ΔL), rolling moment (ΔR), and drag (ΔD) on the follower aircraft. On the other hand, the sidewash v at the vertical tail generates a side force (ΔSF). The changes in these force and moment coefficients,

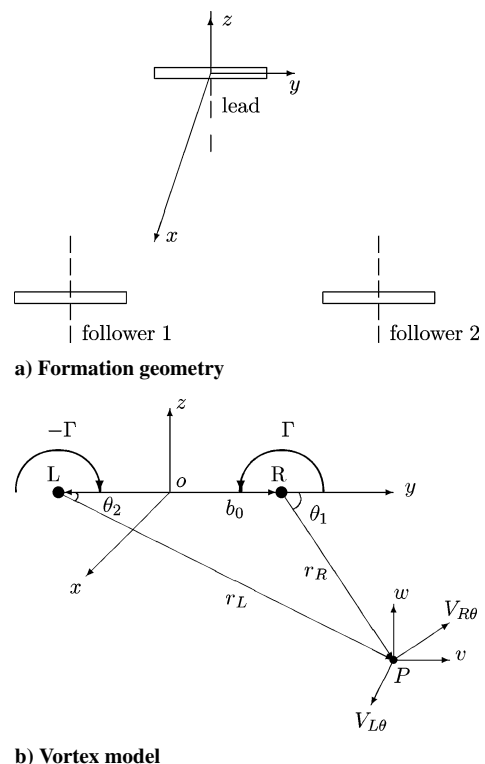


Fig. 1 Schematic of formation flight.

Received 21 October 2004; revision received 15 June 2005; accepted for publication 15 June 2005. Copyright © 2005 by the American Institute of Aeronautics and Astronautics, Inc. All rights reserved. Copies of this paper may be made for personal or internal use, on condition that the copier pay the \$10.00 per-copy fee to the Copyright Clearance Center, Inc., 222 Rosewood Drive, Danvers, MA 01923; include the code 0731-5090/05 \$10.00 in correspondence with the CCC.

*Postdoctoral Fellow, Institute for Aerospace Studies, 4925 Dufferin Street; shan@utias.utoronto.ca.

†Associate Professor, Institute for Aerospace Studies, 4925 Dufferin Street; liu@utias.utoronto.ca. Member AIAA.

Table 1 Parameters of F/A-18 class aircraft

Parameter	Value	Parameter	Value
M , kg	10810	V , m/s	236.0
A , m ²	37.16	h , m	12192
b , m	11.43	ρ , kg/m ³	0.3031
c_R , m	4.04	c_T , m	1.68
AR	3.52	h_z , m	2.7

ΔC_L , ΔC_R , ΔC_D , and ΔC_{SF} , can be calculated as follows:

$$\Delta C_L = \frac{\Delta L}{(1/2)\rho V^2 A} = \frac{C_{L\alpha}}{VA} \int_0^b c(s)w(y+s, z) ds \quad (2)$$

$$\Delta C_R = \frac{\Delta R}{(1/2)\rho V^2 Ab} = \frac{C_{L\alpha}}{VA b} \int_0^b c(s)w(y+s, z) \left(s - \frac{b}{2}\right) ds \quad (3)$$

$$\Delta C_D = \frac{\Delta D}{(1/2)\rho V^2 A} = \frac{C_L + \Delta C_L}{VA} \int_0^b c(s)w(y+s, z) ds \quad (4)$$

$$\Delta C_{SF} = \frac{\Delta SF}{(1/2)\rho V^2 A} = \frac{C_{vt}}{VA} \int_0^{h_z} c_{tail}(s)v(y, z+s) ds \quad (5)$$

where the lift curve slope $C_{L\alpha} = 5.67$ is used,³ C_L is the local lift coefficient, $c(s)$ is the chord distribution along the wing, A is the wing area, C_{vt} is the lift curve slope of the vertical tail, h_z is the tail height, and $c_{tail}(s)$ is a width function of the vertical tail. Moreover, the upwash $w(y+s, z)$ and sidewash $v(y, z+s)$ have the following expressions:

$$w(y+s, z) = \frac{\Gamma}{2\pi} \left[\frac{y+s-b_1}{(y+s-b_1)^2 + z^2 + r_c^2} - \frac{y+s-b_2}{(y+s-b_2)^2 + z^2 + r_c^2} \right] \quad (6)$$

$$v(y, z+s) = \frac{\Gamma}{2\pi} \left[\frac{z+s}{(y+\pi b/8)^2 + (z+s)^2 + r_c^2} - \frac{z+s}{(y-\pi b/8)^2 + (z+s)^2 + r_c^2} \right] \quad (7)$$

with $b_1 = (1 + \pi/4)b/2$ and $b_2 = (1 - \pi/4)b/2$.

When an F/A-18 class aircraft pair in formation flight is considered Fig. 2 shows the induced force and moment coefficients. The parameters of the aircraft are given in Table 1 and taken from <http://www.fas.org/man/dod-101/sys/ac/f-18.htm>. The results show that the optimal relative positions for maximal induced lift are $[y_o, z_o] = [\pm(1 + \pi/4)b/2, 0] = [\pm 10.2 \text{ m}, 0 \text{ m}]$.

The upwash and sidewash also introduce changes in moments on the follower aircraft, including the yawing moment, pitching moment, and the rolling moment. The rolling moment model is introduced here because it is one factor of stability, especially when a large aircraft is followed by a smaller one. If the lead and follower aircraft are the same type, such as the example of three F/A-18s in this Note, flight tests show that the induced moments on the follower are controllable.⁵

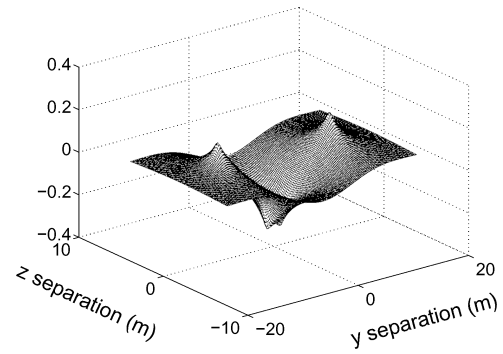
Aircraft Autopilot Models

Each aircraft in formation is equipped with a flight control system that includes three-channel autopilots: Mach-hold, heading-hold, and altitude-hold autopilots²:

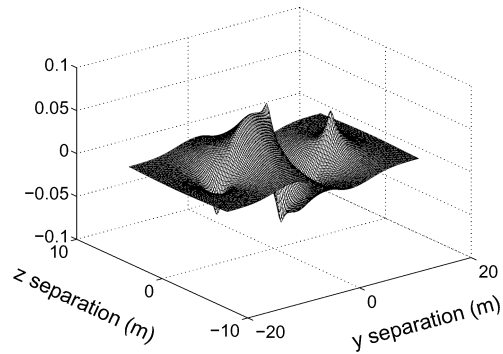
$$\dot{V} = (1/\tau_V)(V_c - V) \quad (8)$$

$$\dot{\psi} = (1/\tau_\psi)(\psi_c - \psi) \quad (9)$$

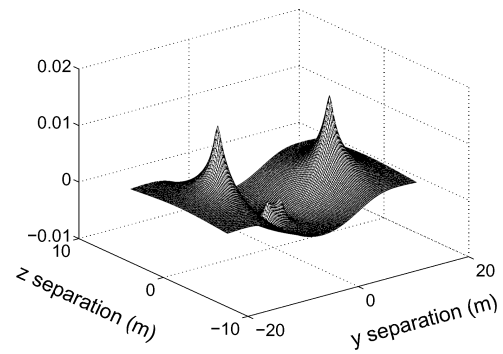
$$\ddot{h} = -[1/\tau_{h_a} + 1/\tau_{h_b}]\dot{h} - (1/\tau_{h_a}\tau_{h_b})h + (1/\tau_{h_a}\tau_{h_b})h_c \quad (10)$$



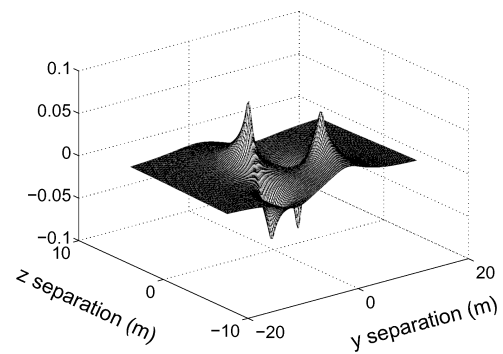
a) Vortex-induced lift coefficient



b) Vortex-induced rolling moment coefficient



c) Vortex-induced drag coefficient



d) Vortex-induced side force coefficient

Fig. 2 Vortex-induced force and moment coefficients.

where subscript c denotes the command for autopilot, ψ is the heading angle, and τ_V , τ_ψ , τ_{h_a} , and τ_{h_b} are the aircraft velocity, heading angle, and two altitude time constants.

These autopilot models make up the basic flight control system for the lead and follower aircraft. They can be directly applied to the lead aircraft. The outer-loop formation flight control system resides on the follower aircraft. It receives measurements of the follower's position relative to the lead aircraft and drives the reference signals of the follower's three-channel autopilots. For the follower aircraft,

the autopilot models need to be modified to take into account the vortex-induced aerodynamic forces by the lead aircraft.

Models for the Follower Aircraft

Applying a similar modification process as that in Ref. 2, we get the following modified autopilot models for the follower aircraft:

$$\dot{V}_F = (1/\tau_V)(V_{Fc} - V_F) + (qA/M)\Delta C_{DFy}(y - y_d) \quad (11)$$

$$\begin{aligned} \dot{\psi}_F &= (1/\tau_\psi)(\psi_{Fc} - \psi_F) \\ &+ (qA/MV)[\Delta C_{SFy}(y - y_d) + \Delta C_{SFz}(z - z_d)] \end{aligned} \quad (12)$$

$$\begin{aligned} \ddot{h}_F &= -[1/\tau_{h_a} + 1/\tau_{h_b}]\dot{h}_F - (1/\tau_{h_a}\tau_{h_b})h_F \\ &+ (1/\tau_{h_a}\tau_{h_b})h_{Fc} + (qA/M)\Delta C_{LFy}(y - y_d) \end{aligned} \quad (13)$$

where subscript F denotes the follower aircraft, $q = \rho V^2/2$ is the dynamic pressure, and ΔC_{DFy} , ΔC_{SFy} , ΔC_{SFz} , and ΔC_{LFy} are the stability derivatives evaluated at the optimal relative position $[y_o, z_o]$. When a design philosophy similar to that in Ref. 2 is obeyed, the induced moments are not incorporated into the design of the outer-loop formation-hold autopilots.

Kinematics for Close-Formation Flight

The kinematics between the follower and the lead aircraft are governed by

$$\dot{x} = -y\dot{\psi}_F - V_F + V_L \cos e_\psi \quad (14)$$

$$\dot{y} = x\dot{\psi}_F + V_L \sin e_\psi \quad (15)$$

where $e_\psi = \psi_F - \psi_L$ is the heading angle error.

Substituting the autopilot models in Eqs. (11–13) into the kinematic equations, we can obtain the following six-dimensional nonlinear equations for the follower aircraft:

$$\begin{aligned} \dot{x} &= -(y/\tau_\psi)(\psi_{Fc} - \psi_F) - (qA/MV)[\Delta C_{SFy}(y - y_d) \\ &+ \Delta C_{SFz}(z - z_d)]y - V_F + V_L \cos(\psi_F - \psi_L) \end{aligned} \quad (16)$$

$$\begin{aligned} \dot{y} &= (x/\tau_\psi)(\psi_{Fc} - \psi_F) + (qA/MV)[\Delta C_{SFy}(y - y_d) \\ &+ \Delta C_{SFz}(z - z_d)]x + V_L \sin(\psi_F - \psi_L) \end{aligned} \quad (17)$$

$$\dot{V}_F = (1/\tau_V)(V_{Fc} - V_F) + (qA/M)\Delta C_{DFy}(y - y_d) \quad (18)$$

$$\begin{aligned} \dot{\psi}_F &= (1/\tau_\psi)(\psi_{Fc} - \psi_F) + (qA/MV)[\Delta C_{SFy}(y - y_d) \\ &+ \Delta C_{SFz}(z - z_d)] \end{aligned} \quad (19)$$

$$\dot{z} = \xi \quad (20)$$

$$\begin{aligned} \dot{\xi} &= -[1/\tau_{h_a} + 1/\tau_{h_b}]\xi - (1/\tau_{h_a}\tau_{h_b})z + (1/\tau_{h_a}\tau_{h_b})h_{Fc} \\ &+ (qA/M)\Delta C_{LFy}(y - y_d) - (1/\tau_{h_a}\tau_{h_b})h_{Lc} \end{aligned} \quad (21)$$

where the control inputs of the lead aircraft, V_L , ψ_L , and h_{Lc} , are considered as disturbances.

Controller Design

A triangular formation-flight configuration, with one lead followed by two followers at right-behind and left-behind, is considered. The control objectives become 1) to maintain the optimal relative positions between the follower and the lead aircraft to obtain the maximal induced lift, even in the face of the lead maneuvers, and 2) to regulate the responses of two followers to achieve synchronous tracking motion.

Linear Proportional–Integral Controller

The linear proportional–integral (PI) controller in Ref. 6 is employed for the tracking control of the follower aircraft. The controller

for the x/y channel contains a linear mixer on the x/y error signals and proportional plus integral action. The z channel controller is a standard PI controller driven by its tracking error. These controllers are

$$V_{Fc_i} = K_{xpi}E_{x_i} + K_{xi} \int_0^t E_{x_i} dt \quad (22)$$

$$\psi_{Fc_i} = K_{ypi}E_{y_i} + K_{yi} \int_0^t E_{y_i} dt \quad (23)$$

$$h_{Fc_i} = K_{zpi}e_{z_i} + K_{zi} \int_0^t e_{z_i} dt + h_{0_i} \quad (24)$$

with

$$E_{x_i} = k_{x_i}e_{x_i} + k_{v_i}e_{v_i} \quad E_{y_i} = k_{y_i}e_{y_i} + k_{\psi_i}e_{\psi_i} \quad (25)$$

where i denotes the i th follower aircraft, $e_{x_i} = x_i - x_{di}$, $e_{y_i} = y_i - y_{di}$, and $e_{z_i} = z_i - z_{di}$ are the relative position tracking errors, $e_{\psi_i} = \psi_{F_i} - \psi_L$ is the heading angle tracking error; $e_{v_i} = V_{F_i} - V_L$ is the velocity tracking error; K_{xpi} , K_{xi} , K_{ypi} , K_{yi} , K_{zpi} , K_{zi} , k_{x_i} , k_{v_i} , k_{y_i} , and k_{ψ_i} are control gains; and h_{0_i} is the initial flight altitude.

Tracking with Synchronization

The cross-coupling concept, which was first introduced in Ref. 7, is employed here to synchronize the relative position tracking motion of two follower aircraft.

First, the position synchronization errors are defined as follows:

$$\varepsilon_{x_1} = e_{x_1} - e_{x_2}, \quad \varepsilon_{x_2} = e_{x_2} - e_{x_1} \quad (26)$$

$$\varepsilon_{y_1} = e_{y_1} - e_{y_2}, \quad \varepsilon_{y_2} = e_{y_2} - e_{y_1} \quad (27)$$

$$\varepsilon_{z_1} = e_{z_1} - e_{z_2}, \quad \varepsilon_{z_2} = e_{z_2} - e_{z_1} \quad (28)$$

Then, the coupled position errors are formed to include both the position tracking errors and the position synchronization errors:

$$e_{x_i}^* = e_{x_i} + \beta_{x_i}\varepsilon_{x_i} \quad (29)$$

$$e_{y_i}^* = e_{y_i} + \beta_{y_i}\varepsilon_{y_i} \quad (30)$$

$$e_{z_i}^* = e_{z_i} + \beta_{z_i}\varepsilon_{z_i} \quad (31)$$

where β_{x_i} , β_{y_i} , and β_{z_i} are positive synchronization gains for the x , y , and z channels of the i th follower aircraft. Hence, the generalized

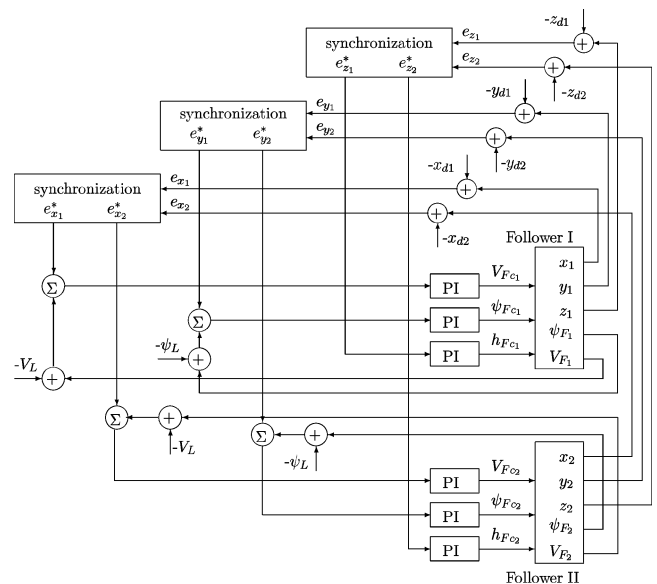


Fig. 3 Structure of control system.

errors for the x and y channels will be

$$E_{x_i}^* = k_{x_i} e_{x_i}^* + k_{v_i} e_{v_i} \quad E_{y_i}^* = k_{y_i} e_{y_i}^* + k_{\psi_i} e_{\psi_i} \quad (32)$$

When E_{x_i} , E_{y_i} , and e_{z_i} in Eqs. (22–24) are substituted by $E_{x_i}^*$, $E_{y_i}^*$, and $e_{z_i}^*$, respectively, the following tracking synchronization controllers are obtained:

$$V_{F_{c_i}} = K_{x_{p_i}} E_{x_i}^* + K_{x_{i_i}} \int_0^t E_{x_i}^* d\tau \quad (33)$$

$$\psi_{F_{c_i}} = K_{y_{p_i}} E_{y_i}^* + K_{y_{i_i}} \int_0^t E_{y_i}^* d\tau \quad (34)$$

$$h_{F_{c_i}} = K_{z_{p_i}} e_{z_i}^* + K_{z_{i_i}} \int_0^t e_{z_i}^* d\tau + h_{0_i} \quad (35)$$

The overall structure of the proposed formation flight controller is shown in Fig. 3. The position tracking errors of two follower aircraft are fed to synchronization blocks to generate the coupled position errors, which are mixed by the heading angle or velocity tracking errors to form the final error signals for the PI controllers.

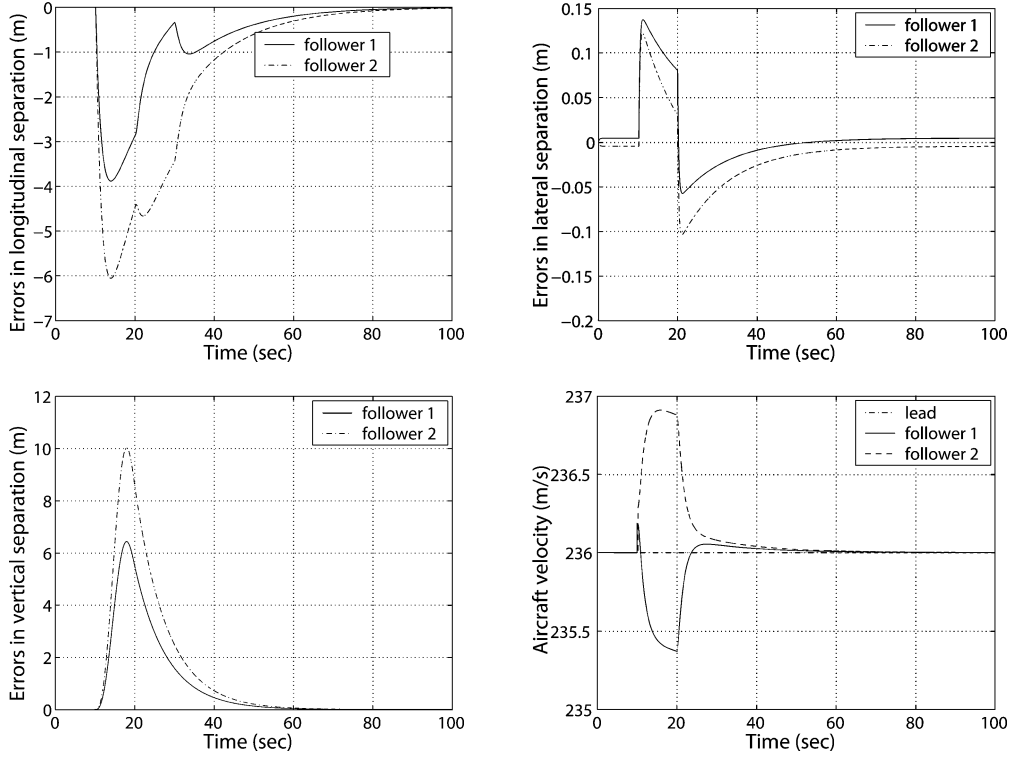


Fig. 4 Formation flight control without synchronization.

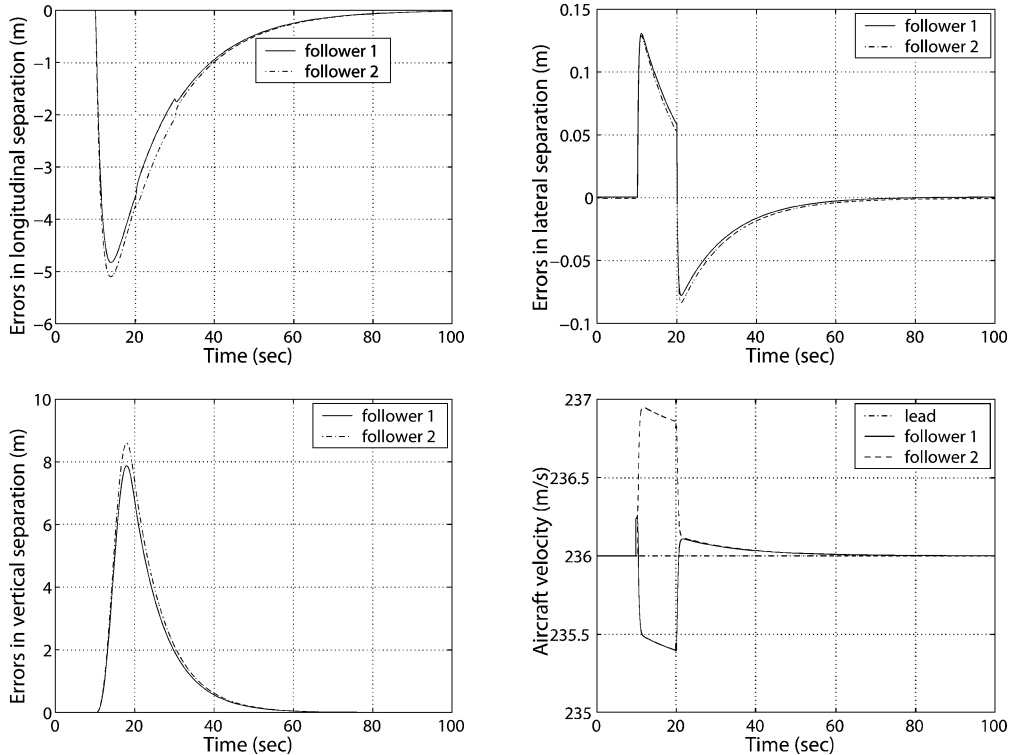


Fig. 5 Formation flight control with synchronization.

Table 2 Vortex-induced stability derivatives

Derivative	Follower 1	Follower 2
ΔC_{LFy}	0.0276	-0.0276
ΔC_{DFy}	0.0033	0.0033
ΔC_{SFy}	0.000849	0.000849
ΔC_{SFz}	0.0018	-0.0018

Table 3 Controller gains for the follower aircraft

Parameter	Value	Parameter	Value
$K_{xp_i}, /s$	3.2	$K_{xi_i}, /s^2$	0.3
$K_{yp_i}, /m$	5.5	$K_{yi_i}, /ms$	0.4
K_{zp_i}	3.0	$K_{zi_i}, /s$	0.25
k_{xi}	-3.0	k_{Vi}, s	6.4
k_{yi}	-1.0	k_{ψ_i}	2.5

Simulation Results

Simulations are performed on the triangular close-formation flight of 3 F/A-18 aircraft. The optimal positions $[x_o, y_o, z_o] = [50.0, \pm 10.2, 0 \text{ m}]$ for maximal induced lift are chosen as the desired relative positions for two follower aircraft to maintain. The longitudinal separation is chosen for safety. The vortex-induced stability derivatives and the controller gains are given in Tables 2 and 3, respectively. The time constants for the follower 1 are chosen to be $\tau_v = 6.0 \text{ s}$, $\tau_\psi = 1.0 \text{ s}$, $\tau_{ha} = 0.5 \text{ s}$, and $\tau_{hb} = 4.1 \text{ s}$, and 95% of those values are applied to follower 2.

At the beginning, two follower aircraft fly in the optimal relative positions with respect to the lead. At 10 s, the lead begins to execute maneuvers: 1) the heading angle maneuvers from 0 to 0.524 rad (30 deg) at a rate of 0.0524 rad/s and 2) the flight altitude changes from 12,192 to 13,192 m at a vertical velocity of 100 m/s. Figure 4 shows the simulation results without synchronization strategy, that is $\beta_{xi}, \beta_{yi}, \beta_{zi} = 0$. Three relative positions and the aircraft velocity achieve asymptotic tracking, although the obvious differences between the tracking errors of two followers can be observed. On the other hand, Fig. 5 shows the simulation results with the synchronization strategy, that is, $\beta_{xi}, \beta_{yi}, \beta_{zi} = 1$. In this case, both followers achieve the asymptotic relative position tracking. In addition, the differences between the relative position tracking errors of two followers have been largely reduced. In other words, these two fol-

lowers form the close-formation flight with the lead aircraft in a more "synchronized" pattern.

Conclusions

The linear synchronized PI controller was developed for the follower aircraft to track their optimal relative positions with respect to the lead. The synchronized motion between two follower aircraft was achieved by using the crossing-coupling concept. This synchronization strategy was combined with the linear PI controller to form an outer-loop synchronized tracking controller. Simulation results of three F/A-18s in a triangular formation flight demonstrated the effectiveness and performance improvement with the proposed synchronization strategy. In this Note, attention was confined to the induced aerodynamic forces due to the outer-loop control structure. Further work is being undertaken to include both the inner-loop and the outer-loop controller design.

Acknowledgments

The authors thank K. B. Ariyur and P. Binetti for their valuable discussions in vortex modeling. The authors also appreciate the anonymous reviewers' constructive comments and suggestions.

References

- ¹Brown, D., "Flight Testing," *Aerospace America*, Vol. 40, No. 12, 2002, pp. 30, 31.
- ²Pachter, M., D'Azzo, J. J., and Proud, A. W., "Tight Formation Flight Control," *Journal of Guidance, Control, and Dynamics*, Vol. 24, No. 2, 2001, pp. 246–254.
- ³Binetti, P., Ariyur, K. B., Krstic, M., and Bernelli, F., "Formation Flight Optimization Using Extremum Seeking Feedback," *Journal of Guidance, Control, and Dynamics*, Vol. 26, No. 1, 2003, pp. 132–142.
- ⁴Binetti, P., Automatic Control of Maximum Efficiency Formation Flight with Fast Extremum Seeking (FES), M.S. Thesis, Faculty of Engineering, Politecnico di Milano, Milan, Italy, June 2001.
- ⁵Hansen, J. L., and Cobleigh, B. R., "Induced Moment Effects of Formation Flight Using Two F/A-18 Aircraft," NASA TM-2002-210732, Aug. 2002.
- ⁶Pachter, M., D'Azzo, J. J., and Veth, M., "Proportional and Integral Control of Nonlinear Systems," *International Journal of Control*, Vol. 64, No. 4, 1996, pp. 679–692.
- ⁷Koren, Y., "Cross-Coupled Biaxial Computer Controls for Manufacturing Systems," *Journal of Dynamic Systems, Measurement and Control*, Vol. 102, No. 2, 1980, pp. 256–272.